Concentration normalization with a model of gain control in the olfactory bulb

B. Raman and R. Gutierrez-Osuna
Department of Computer Science, Texas A&M University, College Station, Texas, USA
{barani, rgutier}@cs.tamu.edu

Abstract

This article presents a biologically-inspired model to remove concentration effects from the multivariate response of a gas sensor array. The model is based on the first stage of lateral inhibition in the olfactory bulb, mediated by periglomerular interneurons. To simulate inputs to the olfactory bulb, sensor-array data are processed with a self-organizing model of chemotopic convergence proposed earlier, which leads to odor-specific spatial patterning. Subsequently, a shunting lateral inhibitory network, modeled after the role of periglomerular cells, compresses the concentration information. The model is validated using experimental data from an array of temperature-modulated metal-oxide sensors.

1. Introduction

The input to the olfactory bulb is characterized by massive convergence of olfactory receptor neuron (ORN) axons expressing the same receptor gene onto a single or few target glomeruli [1]. This chemotopic convergence creates compact odor maps that decouple odor quality from intensity. The encoded intensity information at this early stage is transformed by a layer of lateral inhibitory circuits driven by periglomerular interneurons. These lateral interactions are known to be shunting-type (divisive inhibition), and have been hypothesized to serve as a "volume control" mechanism [2], enabling the identification of odorants over several log units of concentration.

In this paper, we present a computational model of the gain control circuits in the olfactory bulb, and show that the spread of the shunting lateral inhibitions can be used to control the degree of concentration removal performed by the network. We validate the use of the proposed model to perform concentration normalization of signals from an array of temperature-modulated metal-oxide gas sensors.

2. Model

A fundamental difference between machine and biological olfaction is the dimensionality of the input space. The biological olfactory system employs a large population of ORNs (100 million neurons in the human olfactory epithelium, replicated from 1,000 primary receptor types), whereas its artificial analogue uses very few sensors. In order to narrow this dimensionality gap, we exploit the temperature-selectivity dependence of metal-oxide (MOS) materials [3]. Specifically, we modulate the operating temperature of a MOS sensor with a slow (mHz) sinusoidal waveform, and treat the sensor response at each temperature set-point as a "pseudo-sensor."

To model the chemotopic convergence of ORNs onto glomeruli, we perform a topological clustering of the resulting pseudo-sensors according to their selectivity. Formally, we define the selectivity of a pseudo-sensor by its response across a set of C volatile compounds as follows:

$$ORN_i = \left[ORN_i^{O_1},\ ORN_i^{O_2},...,ORN_i^{O_C} \right] \qquad (1)$$

where ORN_i^O is the response of ORN_i to odor O, and C is the number of odorants. We will refer to this C-dimensional space as the affinity space.

The probability distribution of pseudo-sensors in this affinity space is then modeled with a Kohonen Self-Organizing Map (SOM) [4], whose nodes can be considered as virtual glomerular units. Once the SOM is trained, each pseudo-sensor is finally assigned to the closest SOM node in affinity space, thereby forming a convergence map from which the response of each glomerulus can be computed as:

$$G_j^O = \sum_{i=1}^{N} W_{ij} R_i^O \qquad (2)$$

where R_i^O is the response of pseudo-sensor i to odorant O, N is the number of pseudo-sensors, and W_{ij}=1 if pseudo-sensor i converges to SOM node j and zero otherwise.

Shunting lateral inhibition by periglomerular interneurons is modeled as follows:

$$\frac{dx_i^O}{dt} = -Dx_i^O + (B - x_i^O)G_i^O - x_i^O \sum_{k \neq i} c_{ki} G_k^O \qquad (3)$$

where G_i^O is the activity of SOM node i (i.e., after chemotopic convergence), x_i^O is the corresponding neuron output to odor O, $-Dx_i^O$ is a decay term that models the dynamics of a neuron, $\left(B - x_i^O\right)G_i^O$ is the shunting self-excitation, B is the maximum activity of neuron ($0 \le x_i^O \le B$), and $-x_i^O \sum_{k \neq i} c_{ki} G_k^O$ is the shunting inhibition from other neurons [5].

The connection matrix C modeling the shunting inhibition is set as follows:

$$c_{ki} = \begin{cases} U(0,1) & d(k,i) < \dfrac{\sqrt{M}}{r} \\ 0 & otherwise \end{cases} \quad (4)$$

where $U(a,b)$ is a uniform distribution between a and b, and d is the distance between units measured as a Euclidean distance within the lattice ($d = \sqrt{(row_k - row_i)^2 + (col_k - col_i)^2}$; *row* and *col* being the row and column coordinates of a neuron in the lattice), M is the number of SOM nodes, and r determines the width of the lateral inhibitory connections. Self-connections are disabled ($c_{ii}=0$).

It can be shown that the steady-state output of each neuron is:

$$x_i^O = \frac{BG_i^O}{D + G_i^O + \sum_{k \neq i} c_{ki} G_k^O} \quad (5)$$

which, when $c_{ki}=1 \ \forall \ k,i$, and the parameter D=0, becomes proportional to the (L1) normalized response of its input relative to the total network activity:

$$x_i^O = \frac{BG_i^O}{\sum_{\forall k} G_k^O} \quad (6)$$

The original study by Grossberg [5] only considered global connections for the purpose of pattern normalization. However, in this work, we show that by adjusting the spread of the lateral inhibitiory connections using equation (4), the degree of concentration normalization can be controlled parametrically.

3. Results

To validate the model, we have collected a database of temperature-modulated sensor patterns for three analytes: acetone (A), isopropyl alcohol (B) and ammonia (C), at three different concentrations. Three replicas were sampled for each combination of analyte and concentration. Two Figaro MOS sensors (TGS 2600, TGS 2620) [6] were temperature modulated using a sinusoidal heater voltage (0-7 V; 2.5min period; 10Hz sampling frequency). The response of the two sensors (concatenated) to the three analytes at the three concentration levels (three repetitions each) is shown in Figure 1. Each point in the temperature cycle is considered as a separate pseudo-sensor, thus resulting in a population of 3,000 pseudo-sensors.

The population of pseudo-sensors thus generated is projected onto a GL layer with 400 nodes, arranged as a 20x20 SOM lattice, based on the convergence model. Only the sensor response to the highest concentration of each analyte was used to generate the SOM convergence map. Figure 2 shows the odor maps that result from presenting the trained SOM with the sensor response in Figure 1 (only one repetition is shown). It can be clearly seen that the identity of the odor is encoded by a unique spatial pattern across SOM nodes, whereas concentration is related to the intensity and spread of this pattern.

The PCA scatterplot of activity across the network is shown in Figure 3. Without shunting inhibition (a), the model preserves most of the concentration information. With global inhibition (c), the network is able to remove most of the concentration information and provide maximum separability between odors. Different degrees of cancellation can be achieved by controlling the spread of the shunting lateral inhibitory connections (for e.g., refer Figure 3(b)). A detailed characterization of the model is presented in the next section.

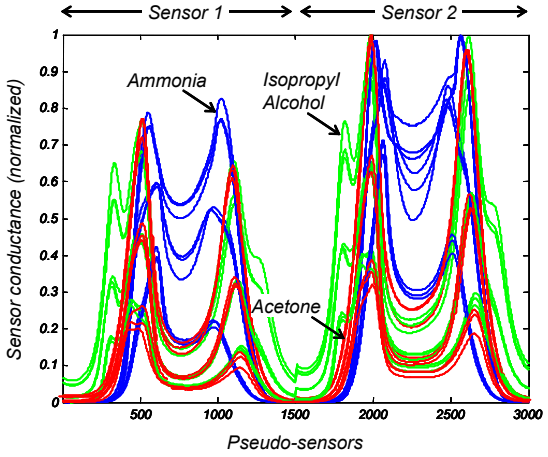

Figure 1. Temperature modulated response of two Figaro MOS sensors to three analytes at three concentrations (three samples each).

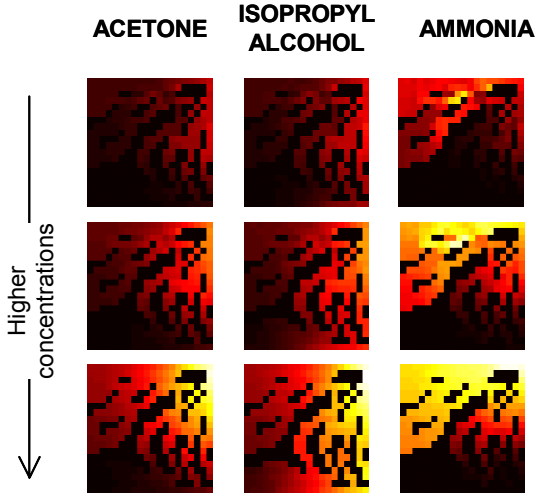

Figure 2. Spatial odor maps generated by chemotopic convergence of 3,000 pseudo-sensors onto a 20x20 SOM. Activity of each GL is normalized by the number of ORNs that converge to it.

4. Characterization of the model

To characterize our model, we employ a measure of separability between categories related to the Fisher's objective function [7]:

$$J = \frac{trace(S_B)}{trace(S_W)} \tag{6}$$

where S_W and S_B are the within-class and between-class scatter matrices, respectively, defined as follows:

$$S_W = \sum_{q=1}^{Q} \sum_{x \in \omega_q} (x - \mu_q)(x - \mu_q)^T \tag{7}$$

$$S_B = \sum_{q=1}^{Q} (\mu_q - \mu)(\mu_q - \mu)^T \tag{8}$$

$$\mu_q = \frac{1}{n_q} \sum_{x \in \omega_q} x \quad and \quad \mu = \frac{1}{n} \sum_{\forall x} x \tag{9}$$

where x is the output pattern of the OB model, Q is the number of odor classes, μ_q and n_q are the mean vector and number of examples for odor q, respectively, n is the total number of examples in the dataset, and μ is the mean vector of the entire distribution. Being the ratio of the spread between classes relative to the spread within each class, the measure J increases monotonically as classes become increasingly more separable.

We define two different measures to quantify concentration-invariant separability and concentration information as follows:

Assuming a three-odor problem, the *concentration-invariant separability* is measured by:

$$J_{odor} = w_1 J_{AB} + w_2 J_{BC} + w_3 J_{CA} \tag{10}$$

where J_{AB}, J_{BC}, and J_{CA} are the separability between odors A and B, B and C, and C and A, respectively, and w_1, w_2, and w_3 are normalization weights to prevent any pair of odors from dominating the metric.

The *concentration information* within each odor class is defined by:

$$J_{conc} = w_4 J_{a1a2a3} + w_5 J_{b1b2b3} + w_6 J_{c1c2c3} \tag{11}$$

where J_{a1a2a3}, J_{b1b2b3}, and J_{c1c2c3} are the separability among the three concentrations within an odor, and w_4, w_5, and w_6 are normalization weights to balance the relative contribution of these three terms. In this paper, the normalization weights are determined so that the maximum value of each term ($w_1 J_{AB}$, $w_2 J_{BC}$, $w_3 J_{CA}$, $w_4 J_{a1a2a3}$, $w_5 J_{b1b2b3}$, $w_6 J_{c1c2c3}$) becomes 1.

4.1 Spread of the lateral connections (r)

Figure 4(a) shows the *concentration-invariant separability* measure (J_{odor}) as a function of the width of the shunting inhibitory connections. Maximum separability between the odors is achieved for small r (global connections). Global connections remove most of the concentration information, a result that follows from the steady-state response in equation (5) and the scatterplot in Figure 3(c). In contrast, reduction in the width of the shunting inhibition allows the within class-scatter to increase, thereby reducing J_{odor}.

Figure 4(b) shows the *concentration information* measure (J_{conc}) as a function of the width of the shunting inhibitory connections. Maximum separability is achieved for no shunting inhibition ($r=20$). In this case concentration information serves as the principal source of variance, as shown in Figure 3(a). As the connections become global, most of the concentration information is removed. In between the two extremes, different degrees of separability can be achieved among concentration levels of the same odor.

The width of the lateral inhibition can therefore be used to provide an appropriate tradeoff between odor class information (between class-scatter) and odor concentration information (within class-scatter).

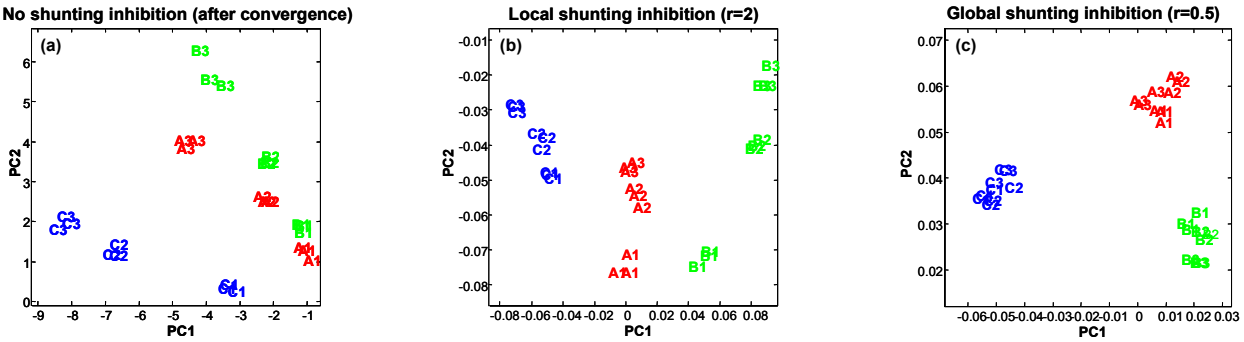

Figure 3. PCA scatterplot of SOM activity following normalization with the shunting inhibition network (A1: lowest concentration of analyte A, C3: highest concentration of analyte C). Model parameters $B=1$, $D=0.1$.

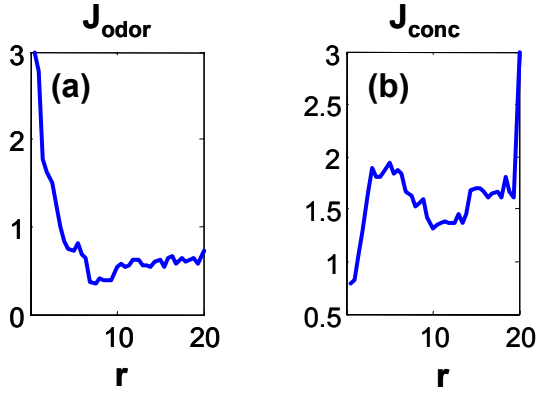

Figure 4. Characterization of the model; small *r* represents global connections and large *r* represents local connections. (a) Measure of concentration-invariant separability (J_{odor}) as a function of the width of shunting lateral inhibition. (b) Measure of concentration information (J_{conc}) as a function of the width of shunting lateral inhibition**.**

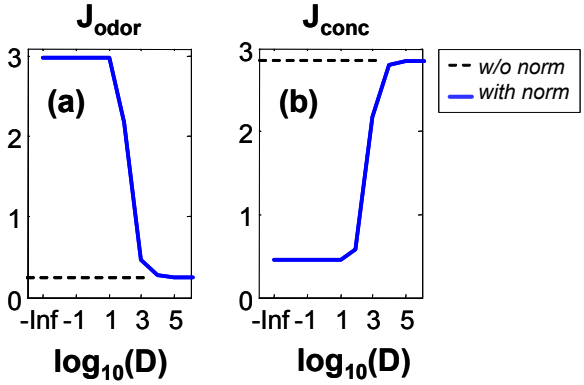

Figure 5. Characterization of the exponential decay rate (D) (a) Measure of concentration-invariant separability (J_{odor}) as a function of the decay parameter *D*. (b) Measure of concentration information (J_{conc}) as a function of the decay parameter *D*. (model parameters $r=0.5$ *and* $c_{ki}=1 \ \forall \ k,i$). Dashed line indicates separability without shunting-inhibition normalization.

4.2 Rate of exponential decay (D)

Figure 5(a,b) shows the *concentration-invariant separability* and *concentration information* measures as a function of decay rate *D*. For small value of *D* ($D << \sum_k G_k^O$), the model achieves concentration compression similar to the L1 norm, thereby improving separability between odors as shown in Figure 5(a). For large *D* values ($D >> \sum_k G_k^O$), the steady state response of the model is a scaled version of its inputs and hence the model retains all the concentration information, as shown in Figure 5(b). Therefore, for a fixed spread of lateral connections, the exponential decay rate *D* can also be used to control the amount of concentration compression.

5. Conclusions

We have presented a neurodynamic model of the first stage of lateral inhibition in the olfactory bulb, mediated by periglomerular interneurons. We have shown that global connections remove most of the concentration information, increasing the separability between odors. Local connections, on the other hand, retain most of the concentration information but do not increase separability between odor classes. By controlling the width of the lateral connections or the rate of decay of the neurons, different degrees of concentration normalization can be achieved.

The next stage in this research is to characterize this normalization process using theoretical dose-response curves for different sensor models including metal oxide sensors, conducting polymer sensors and olfactory receptor neurons.

Acknowledgments

This material is based upon work supported by the National Science Foundation under CAREER award 9984426/0229598. Takao Yamanaka, Agustin Gutierrez-Galvez, Alexandre Perera-Lluna are gratefully acknowledged for valuable suggestions during the preparation of this manuscript.

References

1. Vassar, R., et al., "Topographic Organization of Sensory Projections to the Olfactory Bulb," Cell, Vol. 79 (1994), pp. 981-991.
2. Freeman, W., "Olfactory system: odorant detection and classification," In D. Amit and G.Parisi (eds.), Building blocks for Intelligent Systems: Brain components as Elements of Intelligent Function, Vol. III, part 2, Academic Press (New york, 1999).
3. Lee, A. P., and Reedy, B. J., "Temperature modulation in semiconductor gas sensing," Sensors and Actuators, Vol. B60 (1990), pp. 35-42.
4. Kohonen, T., "Self-organized formation of topologically correct feature maps," Biol. Cybern. Vol. 43, (1982) pp. 59-69.
5. Grossberg, S., "Adaptive Pattern Classification and Universal Recording: I Parallel Development and Coding of Neural Feature Detectors," Biological Cybernetics, Vol. 23 (1976), pp. 121-134.
6. Figaro 1996, Figaro Engineering, Inc., Osaka, Japan.
7. Lei Wang and Kap Luk Chan, "Learning kernel parameters by using class separability measure," 6th Kernel Machine Workshop on Learning Kernels (in conjunction with Neural Information Processing Systems Conference), Whistler, Canada, 2002.